Desalination and Water Treatment
www.deswater.com
doi: 10.5004/dwt.2019.23722

147 (2019) 73–82
April

Design and characterization of a cost-effective cermet membrane: implementation in paper mill wastewater treatment

Mabrouk Ben Hamden[a,*], Gisèle Lecomte-Nana[b], Jamel Bouaziz[a]

[a]*LCI: Laboratory of Industrial Chemistry, National School of Engineering, University of Sfax.BP 1173, 3038 Sfax, Tunisia, Tel. +216 23016780; Fax: +216 74676908; email: benhamdenemabrouk@gmail.com (M.B. Hamden), jamel.bouaziz@gmail.com (J. Bouaziz)*
[b]*ENSCI, IRCER: Institute of Research for Ceramics, European Ceramic Center (UMR CNRS 7315), F-87000 Limoges, France, email: gisele.lecomte@unilim.fr (G. Lecomte-Nana)*

Received 24 September 2018; Accepted 1 January 2019

ABSTRACT

This work aims to produce ceramic-metal composite (cermet) membrane supports based on kaolin and aluminum powders. Flat ceramic membrane supports were prepared from the mixtures of kaolin (K), feldspar (F), sand (S), and two types of aluminum: industrial aluminum waste (Ali) and commercial aluminum (Alc).The samples were obtained by uniaxial pressing with 58.5 MPa in cylindrical moulds and then sintered at 1,350°C for 2 h in order to obtain flat cermet membrane supports of 30 mm in diameter and 6 mm in thickness. Porosity, permeability, and mechanical properties of these supports were studied as functions of the amount of aluminum powder. These characterizations proved that the addition of 4 wt.% aluminum to a 50% kaolin, 25% feldspar, and 25% sand porcelain matrix has a beneficial effect on the membrane support properties. In particular, the presence of aluminum progressively increased water permeability, porosity, and mechanical strength. The cermet membrane support application in the treatment of wastewater from paper mills shows a significant decrease in turbidity, about 97% retention rate of chemical oxygen demand, and an almost total color removal.

Keywords: Microfiltration; Purification; Aluminum; Ceramic membrane supports; Cermet; Mechanical properties; Permeability

1. Introduction

The development of industrial activity releases various toxic wastes, such as paper mill wastewater, causing, thus, a serious threat to the ecosystem. Moreover, big amounts of aluminum wastes are being rejected from industries daily. Aluminum wastes come from different sources, e.g., aluminum cans, furniture, aluminum foil, aluminum scraps, and appliances [1]. This waste is often called old scrap. To this is added another aluminum waste, called "new scrap" [2]. New scrap originates during the manufacturing of aluminum semifabricated and final products (shavings, offcuts, molded parts, etc.). Because old scrap is collected after disposal from consumers in the form of cables, pots, and radiators, it is necessarily more contaminated than new scrap, and preliminary treatments of the scrap are generally necessary. For this reason, this work focused on using new scrap. It is worth mentioning that the United States of America alone released 20,000 metric tons of this scrap in 2017 [3]. In addition to its purity, the new scrap is generally disposed of as a waste. It would be very beneficial to valorize it in various processes and use it to solve other problems.

Hence, in a first step, studies investigated some properties of the materials required in the membranes used for filtration and separation processes to purify wastewaters. Among these properties were the pore size distribution, the total porosity, the surface quality, the mechanical properties, the chemical stability, and the permeability [4]. For this purpose, ceramics were chosen as a good material that possesses these

* Corresponding author.

characteristics. Indeed, Xu et al. [5] revealed that the membrane made from porous ceramic materials showed high separation selectivity, a low permeation resistance, and good mechanical and separation performances. Furthermore, this composite has the potential of being very efficient in the separation and filtration processes [6–13].

In order to further reduce cost, many researchers have been devoted to fabrication of ceramic membranes using various cheap raw materials such as kaolin [6,7] and fabricated low-cost macroporous membranes for microfiltration applications [9,10,12]. Frang et al. and Nandi et al. [8,13] tested oil-water emulsion using ceramic membrane. However, it was observed that in terms of pore size and mechanical properties, ceramic membranes fell short of meeting the efficiency requirements to purify paper mill wastewater sludge.

For this reason, research turned to designing filtration membrane supports made of ceramics and metals. The implementation of such an idea would solve many problems at once. First, it would valorize the industrial metallic wastes. Second, it would reduce the cost of the membrane. Third, it would improve the filtration performance of the new membrane.

The new composite was called "cermet." The noun of this composite was derived from a combination of the words "ceramics" and "metal," the two major phases of this material. Having a long lifetime and a good thermal and chemical stabilities, cermet combines the mechanical and microstructural properties of both, ceramics and metal.

The preparation of the ceramic/metal composites is generally performed by the synthesis and then the consolidation of powders according to the methods of powder metallurgy process [14]. It was sometimes considered optional to add binders and plasticizers, followed by conventional sintering or uniaxial or isostatic pressing.

However, although there was an abundance of information on cermet instead of pure ceramics for hydrogen separation [15–17], to our knowledge, very little is known on the addition of aluminum as an additive to kaolin, feldspar, and sand to produce cermet membrane supports for paper mill wastewater filtration. In particular, this work intends to assess the effect of the addition of aluminum to ceramics to obtain cermet membranes. It would be very important to compare the impact of using the commercial aluminum (Alc) and that of industrial aluminum (Ali), and particularly new scrap, in terms of membrane pore size and mechanical behavior. It was expected that aluminum plays a triple advantage. First, it would increase the porosity of the elaborated composite, which would enhance the performance of the membrane supports during the filtration of the paper mill wastewater. Second, it would improve its mechanical strength and increase its longevity. Third, the use of Ali as an additive would especially present a two-fold advantage. It would alleviate the impact of old scrap on the environment and produce a cost-effective product.

2. Materials and methods

2.1. Materials and chemicals

In this study, the used raw materials were (1) kaolin (K), feldspar (F), and sand (S) provided by GARTHAGO CERAMIC, Ltd, Sfax, Tunisia, (2) two types of aluminum, Ali waste in the form of new scrap collected from metal manufacturing industry in the region of Sfax, Tunisia, and Alc in the form of commercial powder (Alc) acquired from Fluka, Spain. The chemical composition, determined by inductively coupled plasma analysis, is summarized in Table 1. The major elements, assumed as oxides, present in kaolin were SiO_2 and Al_2O_3. The amounts of Fe_2O_3 and K_2O were higher than those of Na_2O. Sand consisted of SiO_2 as major constituent, as expected, with Na_2O as the main associated oxide. The major components present in feldspar were Al_2O_3 and SiO_2. As can be clearly observed, the main impurities were K_2O, Na_2O, and CaO.

Table 2 shows the main characteristics of the Alc powder used in this study. As can be clearly seen, its purity is greater than 99%.

Table 3 exhibits the chemical composition of the Ali waste revealed by the X-ray fluorescence technique. As can be seen, this material contained 92.52% of aluminum. The rest was made of impurities of Ca, Ti, Si, Fe, and Mn derived from surface contamination with oxides and machining oil [18,19].

The kaolin particle size distributions, feldspar, sand, and aluminum were determined. Fig. 1 shows the average particle size of all the materials. It ranged between 7.1 and 142.1 μm.

2.2. Elaboration of membrane supports

A paste was obtained by mixing a ceramic powder with water. The paste was characterized in function of following

Table 1
Chemical composition (mass %) of raw materials

Oxides	SiO_2	Al_2O_3	K_2O	Fe_2O_3	Na_2O	CaO	L.O.I*
K	48.47	36.43	0.97	0.88	0.63	–	12.07
F	79	12.45	2.8	–	4.58	0.47	0.6
S	94.58	0.93	0.29	–	3.81	–	0.36

*L.O.I: loss on ignition at 1,000°C.

Table 2
Characteristics of the commercial aluminum powder used

Granulometry	100–200 μm
Density (g cm^{-3})	2.7
Purity	>99%

Table 3
Chemical composition (mass %) of industrial aluminum waste

Compound	Ali
Al	92.52
Ca	1.58
Ti	2.49
Si	1.71
Fe	0.79
Mn	0.46

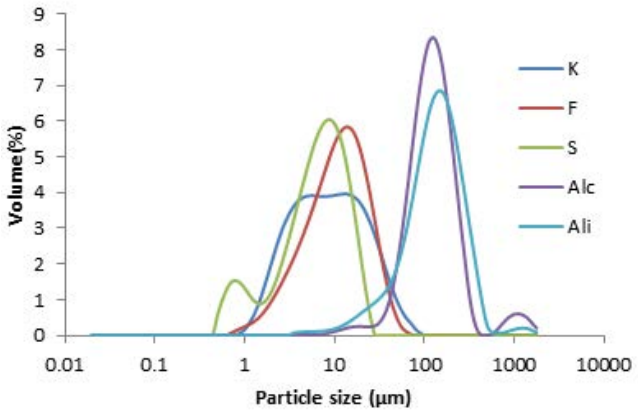

Fig. 1. Particle size distributions of the used kaolin, feldspar, sand, and aluminum.

qualities: plasticity, homogeneity, hardness, and cohesion. This procedure adopted the following steps.

First, the raw materials were mixed dry in order to ensure a good homogeneity of the mixture. Second, after drying, a wet mixture was made by adding distilled water and hydrochloric acid to adjust the pH to 4 while kneading until a plastic paste was obtained. Third, the dough was dried at 110°C during 24 h. Fourth, the homogeneous raw ceramic clods were finely crushed using a mortar. Fifth, the powders of each clay mixture were dried and pressed at 58.5 MPa. Cylindrical pellets of 30 mm in diameter and 6 mm in thickness were produced. Finally, the pellets were sintered using a programmable furnace at 1,350°C with a heating rate of 5°C min^{-1} for 2 h.

2.3. Characterization techniques

Different techniques were adopted for the characterization of the raw materials and the prepared membrane supports, namely, the particle size distribution, X-ray diffraction (XRD), the differential thermal analysis (DTA), the thermogravimetric analysis (TGA), dilatometric analysis, mechanical strength, Young's modulus, chemical resistance, total porosity, mercury intrusion porosimetry, water permeability, and scanning electron microscopy (SEM).

The particle size distribution was measured using the laser particle size analysis (MASTERSIZER 2000). The test was conducted in water suspension. In order to avoid flocculation, samples were ultrasonicated for 5 min.

XRD diagrams were obtained on powdered samples with a "D8 Bruker Advance" powder diffractometer using Kα1 radiation of Cu (λ = 0.15406 nm). XDR experiments were achieved in step-scan mode from 0° to 60° (2θ). Quantification of the different phases was conducted using the computer program X'-pert High Score.

DTA and TGA were carried out from ambient temperature to 1,350°C with a rate of 10°C min^{-1}under air, using a Setaram instrument (SETARAM Setsys 24 apparatus, France).

The SEM was performed on the flat polished surface to ensure investigation on the real bulk structure of the specimens. The microstructure was analyzed using the Phillips XL 30 SEM working with 15 kV accelerating voltage.

Linear shrinkage was determined with dilatometry analysis using a SETARAM Setsoft 2000 apparatus (France) at a heating rate of 10°C min^{-1} between ambient temperature and 1,200°C, under dry air atmosphere of samples (6 mm in diameter and 5 mm in thickness) pressed at 25 MPa from the powder fractions of 63 µm.

The tensile strength of the different cermet supports was calculated using a LLOYD EZ50 Instrument, measured by the Brazilian test applied to sintered flat disks with a displacement rate of 0.5 mm min^{-1}. The maximum rupture strength σ_r (MPa) was determined following the elasticity theory [20]:

$$\sigma_r = \frac{2P_{max}}{\pi LD} \quad (1)$$

where L (mm) and D (mm) are the sample length and diameter, respectively. P_{max} (N) is the maximum applied load recorded at failure. Three samples of each composition elaborated under the same conditions were tested, and an average value was then calculated.

The chemical corrosion resistance was conducted using aqueous solutions of nitric acid [0.45 M] and sodium hydroxide [0.5 M] at room temperature for 8 d. All the samples were rinsed in distilled water and dried at 110°C. The degree of corrosion was evaluated by the percentage of the weight loss.

The porosity of the sintered composites was determined by helium pycnometer (Micrometrics, Accupys//1340 Gas pycnometer, USA). Four specimens were selected to determine porosity with an error of less than 1% of the measured porosity value.

The pore size distribution of the sintered ceramic supports was determined by a mercury intrusion porosimetry method (Micromeritics, Model Auto pore 9500, France).

The turbidity was measured using a Turbidimeter HACH RATIO 2100 A.

Fig. 2 exhibits the laboratory setup made from glass (filtration cell type AMICON) used in this study for liquid permeation experiments. The support with a filtration area of 7 cm^2 and a thickness of 6 mm was placed in the membrane

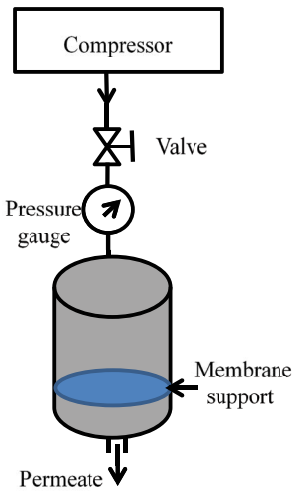

Fig. 2. Scheme of the pilot plant.

housing, and water was poured into the system from the top. All filtration experiments were conducted at a temperature of 25°C ± 2°C. Being a very important parameter for characterizing membrane filtration, hydraulic permeability was estimated from Darcy's law according to the equation:

$$J = L_p \Delta P \quad (2)$$

with L_p representing the hydraulic permeability of the membrane (L h^{-1} m^{-2} bar^{-1}) and ΔP representing the transmembrane pressure (TMP) calculated in bar.

2.4. Compositions

Table 4 summarizes the composition of the various samples.

3. Results and discussion

3.1. Characterization of the starting materials

The XRD diagrams of the raw materials are represented in Fig. 3. The characteristic peaks of the minerals are indicated on the diagram. Kaolin is mainly constituted of kaolinite, illite, and quartz. It can be clearly observed that all sand diffraction peaks can be identified as a quartz phase since there is no other detectable phase. Feldspar is mainly made up of albite, orthoclase, and illite.

Figs. 4 and 5 display the XRD patterns of the two types of Alc and Ali. Both aluminums are pure. The presence of only aluminum peaks in the XRD diffractograms confirmed the purity of the material.

Table 4
Compositions and sample designations of the supports

Sample label	K (wt.%)	F (wt.%)	S (wt.%)	Alc or Ali (wt.%)
Support 0	50	25	25	0
Support 4	48	24	24	4
Support 7	46.5	23.25	23.25	7
Support 10	45	22.5	22.5	10
Support 15	42.5	21.25	21.25	15
Support 20	40	20	20	20

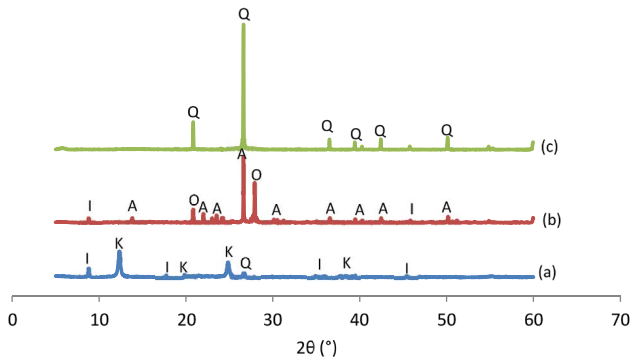

Fig. 3. XRD diffractograms of the kaolin (a), the feldspar (b), and the sand (c). Legend: Q: quartz, A: albite, K: kaolinite, I: illite, and O: orthoclase.

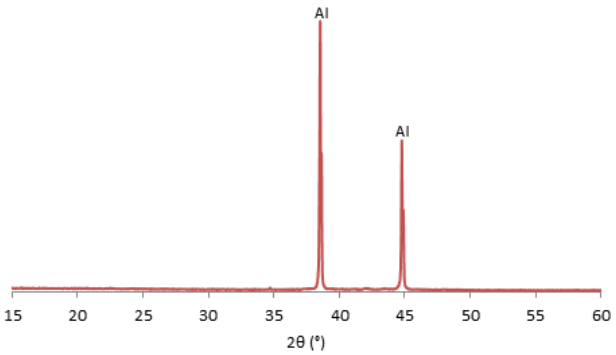

Fig. 4. XRD diffractogram of the Alc powder.

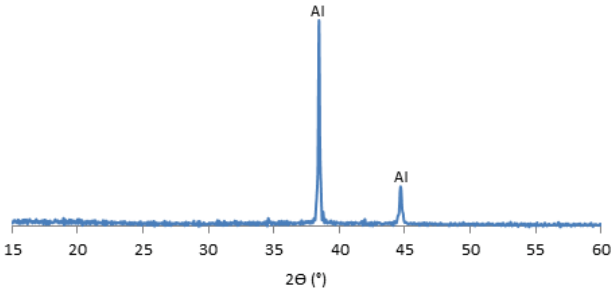

Fig. 5. XRD diffractogram of the Ali powder.

The XRD diagrams of composites are shown in Fig. 6. Before heat treatment, the samples mainly consisted of kaolinite, illite, albite, quartz, and aluminum. At a temperature of 1,350°C for 2 h, all the peaks referring to kaolinite, illite, and albite disappeared and a new peak of mullite was detected. This mullite formation is first attributed to the reaction between metakaolinite, feldspar, and sand. On the other hand, it was probably ascribed to the reaction of α-alumina with the metakaolinite.

Figs. 7 and 8 illustrate the DTA-TGA analysis curves of the mixtures with 0 wt.% aluminum, with 4 wt.% Alc and with 4 wt.% Ali. The TGA curve of the mixture with 0 wt.% aluminum shown in Fig. 8(a) exhibits the total weight loss of about 7% taking place in two stages. The first one is considered as a slight weight loss occurring between room temperature and 150°C. It can be explained by the removal of the adsorbed water. The second one occurring at the temperature range between 400°C and 600°C would be mainly caused by the dehydroxylation of the kaolinite.

The DTA thermogram displayed in Fig. 7(a) shows two endothermic peaks at 100°C and 550°C associated with the two stages of weight loss. The endothermic effect which occurred at 573°C can be attributed to the transformation of quartz α to quartz β. However, in line with Yamuna et al. [21], the exothermic peak at 980°C without any weight loss would be very likely assigned to the crystallization of spinel or mullite.

It is worth observing that the mixture with 0 wt.% aluminum always lost around 7% of its weight under the effect of heat. However, the total weight loss of the mixture with 4 wt.% Alc was reduced to 6%, whereas the total

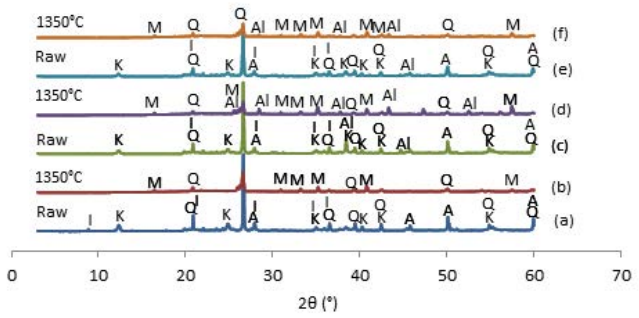

Fig. 6. XRD diffractograms of the mixtures before and after heat treatment (Support 0 (a), Support 0 (b), Support 4 Alc (c), Support 4 Alc (d), Support 4 Ali (e), and Support 4 Ali (f)) Legend: Q: quartz, Al: aluminum, K: kaolinite, I: illite, M: mullite, A: albite.

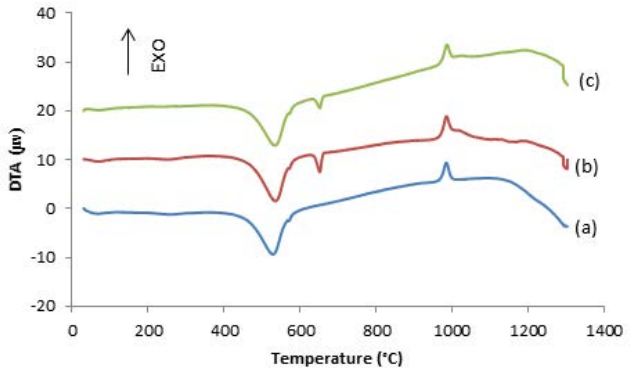

Fig. 7. DTA curves of the mixture (0 wt.% aluminum) (a), 4 wt.% Alc (b), and 4 wt.% Ali (c).

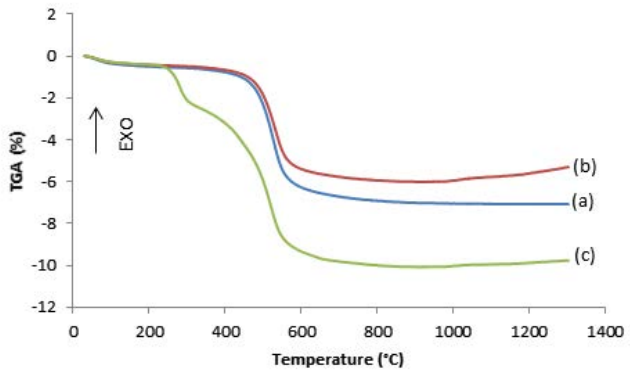

Fig. 8. TGA curves of the mixture (0 wt.% aluminum) (a), 4 wt.% Alc (b), and 4 wt.% Ali (c).

loss of the mixture with 4 wt.% Ali was amplified to about 10% which was attributed to the decomposition of organic matter present in the aluminum waste. Therefore, it can be inferred that the addition of aluminum powder to the mixture modified its thermal behavior. The DTA curves of the mixtures with 4 wt.% Alc and Ali shown in Figs. 7(a) and 7(b) revealed the existence of two phases. The first one would represent the solid-state oxidation of aluminum, starting at ~600°C and ending at 660°C, the melting point of aluminum. The second phase would represent the liquid-state oxidation of aluminum occurring at temperatures between 660°C and ~1,020°C. This is in total agreement with previous findings by other authors [22–23].

The dilatometric behavior of the mixtures is plotted in Fig. 9. The first shrinkage, occurring between room temperature and 120°C, can be explained by the reduction of the adsorbed water while the thermal expansion detected at 573°C would be due to the polymorphic α-β transition of quartz. The second shrinkage occurring at 975°C would be explained by a structural reorganization and the beginning of densification.

3.2. Characterization of the elaborated supports

The flat membrane supports were elaborated by uniaxial pressure molding. We attempted to study the influence of experimental conditions on the performance of elaborated membrane supports.

3.2.1. Mechanical strength

Fig. 10 shows that the rupture strength changed in function of the quality of aluminum. This curve reveals

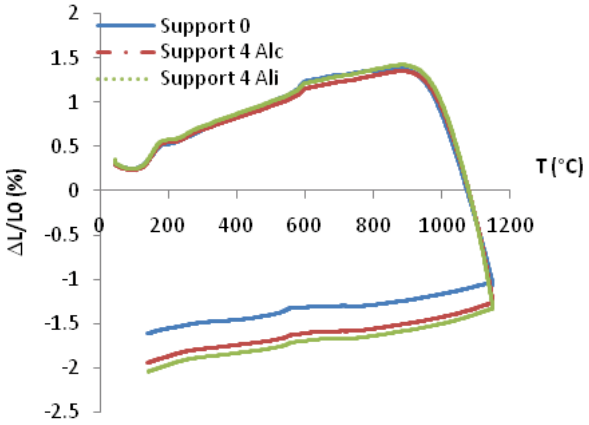

Fig. 9. Linear shrinkage versus temperature of the mixture (0 wt.% aluminum), 4 wt.% Alc, and 4 wt.% Ali (heating and cooling rates of 10°C min^{-1}).

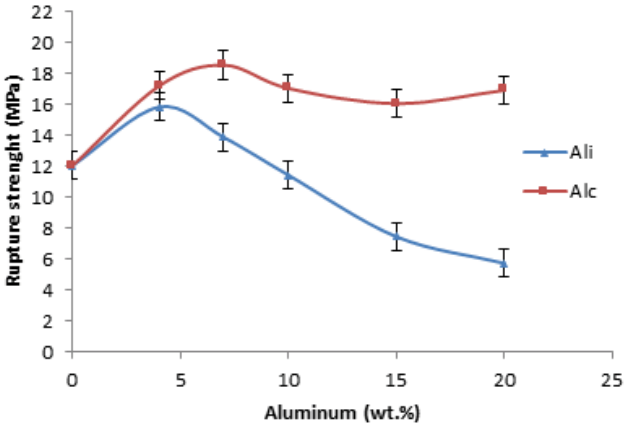

Fig. 10. Rupture strength of the samples with different wt.% of aluminum sintered at 1,350°C for 2 h.

that the rupture strength increased to reach a maximum value of 15.8 MPa for a mixture with 4% of Ali and 18.6 MPa for a mixture with 7% of Alc. Then, the curve shows clearly that this rupture strength differs for the two mixtures. Indeed, with percentages of Ali superior to 4%, the rupture strength gradually decreases to reach 5.74 MPa at an addition of 20% Ali. While with Alc percentages superior to 7%, the rupture strength decreases slightly to reach 17 MPa at an addition of 20% Alc. As was explained by previous researchers [24], this difference in the behavior of the cermet can be explained by the increase of H_2 gas formation creating foams from the dissolution of aluminum in water-based suspensions, which promotes the fragility of the ceramic supports.

3.2.2. Young's modulus

The evolution of Young's modulus of the samples sintered at 1,350°C for 2 h with different percentages of aluminum is illustrated in Fig. 11. Young's modulus reached its optimum value of 34.7 GPa with the mixture containing 4 wt.% of Alc. Similarly, it reached its optimum value of 21.8 GPa with a mixture containing the same percentage of Ali.

3.2.3. Chemical resistance

The supports sintered at 1,350°C for 2 h were soaked at room temperature in HNO_3 and NaOH solutions. The results reported in Figs. 12 and 13 show that both support membranes with Ali and Alc presented a good chemical resistance in HNO_3. Indeed, After 8 d of immersion in the acid medium, the weight loss did not exceed 0.18% and 0.3% for Alc and Ali, respectively. However, it reached 0.45% and 0.75% for the respective materials in NAOH. In addition, it can be clearly seen that the membranes containing Alc showed a better resistance to corrosion in both media than membranes containing Ali.

3.2.4. Total porosity

Fig. 14 exhibits the total porosity of the samples with different wt.% of Ali and Alc at 1,350°C for 2 h. The first result

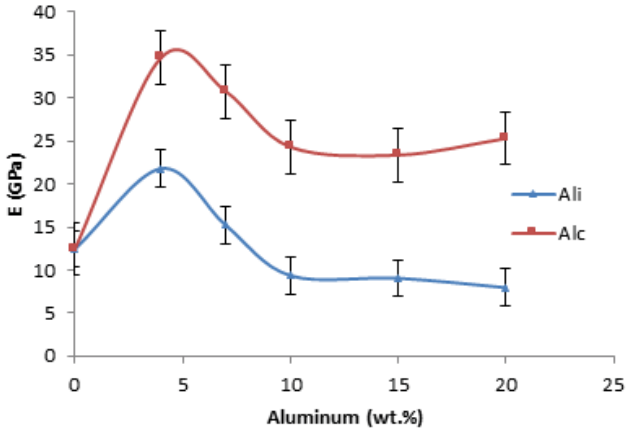

Fig. 11. Young's modulus of the samples with different wt.% of aluminum sintered at 1,350°C for 2 h.

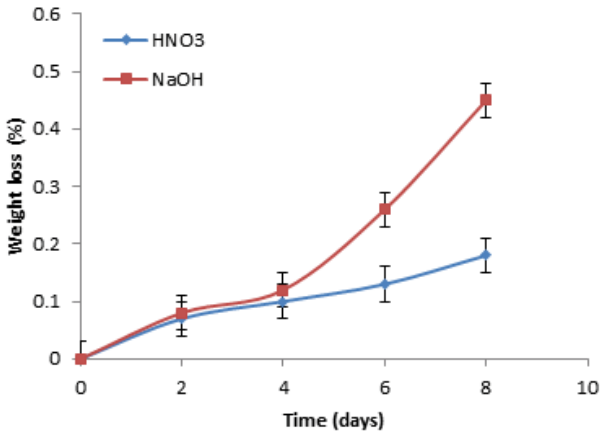

Fig. 12. Weight loss of supports containing 4 wt.% of Alc sintered at 1,350°C for 2 h in HNO_3 and NaOH as a function of time.

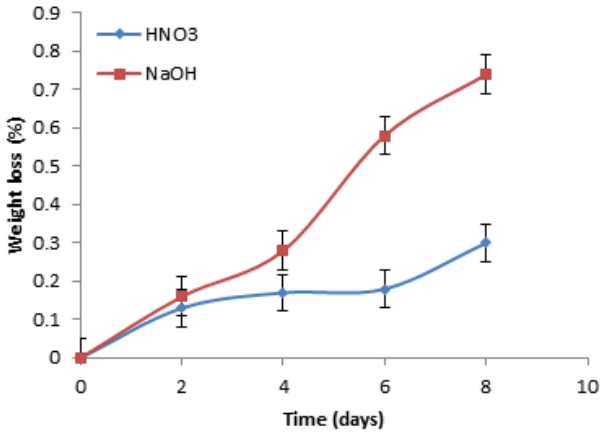

Fig. 13. Weight loss of supports containing 4 wt.% of Ali sintered at 1,350°C for 2 h in HNO_3 and NaOH as a function of time.

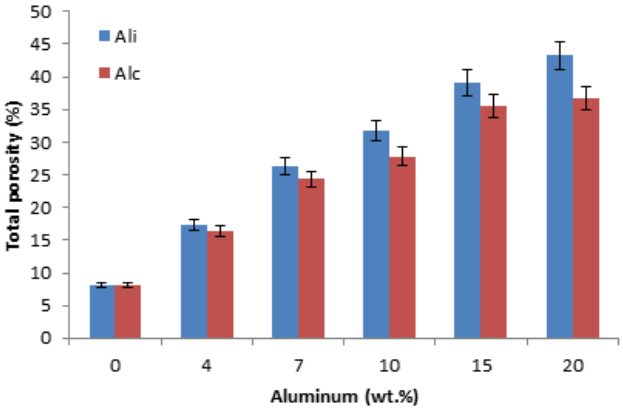

Fig. 14. Total porosity of the samples with different wt.% of aluminum sintered at 1,350°C for 2 h.

of importance was that the membranes with Ali showed a higher porosity than those with Alc. Second, it was clearly observed that the porosity showed a positive relation with the amount of aluminum added. Indeed, the more percentage

of metal added to the mixture resulted in greater porosity. In line with ref. [22], this can be explained by the bigger voids and pores created during the exothermic oxidation reaction of aluminum.

3.2.5. Mercury intrusion porosimetry

The pore size distribution curves of the fabricated porous cermet supports sintered at 1,350°C for 2 h are reported in Figs. 15 and 16. Results indicate that flat ceramic supports elaborated with aluminum encompass bimodal pore size distribution. This is typical of the presence of macropores. Indeed, the pores size distributions were moderately large, varying from 10 to 200 μm with mean diameters of approximately 147 and 184 μm for ceramic supports containing 4 wt.% Alc and 4 wt.% Ali, respectively. These results could be explained by the oxidation of aluminum to form hydrogen responsible for the formation of pores [22].

3.2.6. Scanning electron microscopy

The SEM micrographs of the membrane sintered at 1,350°C for 2 h with and without aluminum are reported in Fig. 17. Typical illustrations of the heterogeneous microstructures reveal the presence of large pores and spherical cavities. These cavities were created during the oxidation of aluminum and occupied the locations of initial aluminum grains. Consequently, the pore size increased with the addition of aluminum content. The oxidation of aluminum occurs in the liquid phase due to the large particle size (Ø > 100 μm). This result explains the presence of spherical porosity in the microstructure.

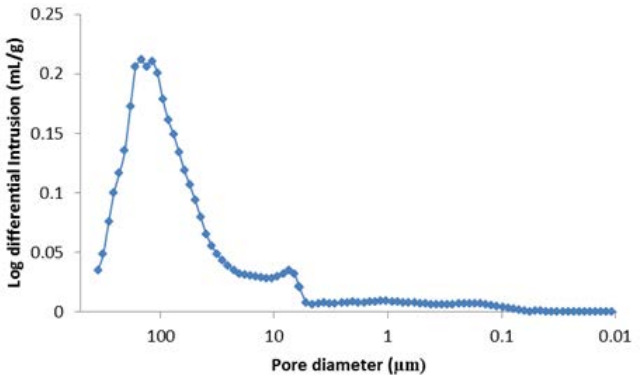

Fig. 15. Pore size distribution of supports containing 4 wt.% of Ali sintered at 1,350°C for 2 h.

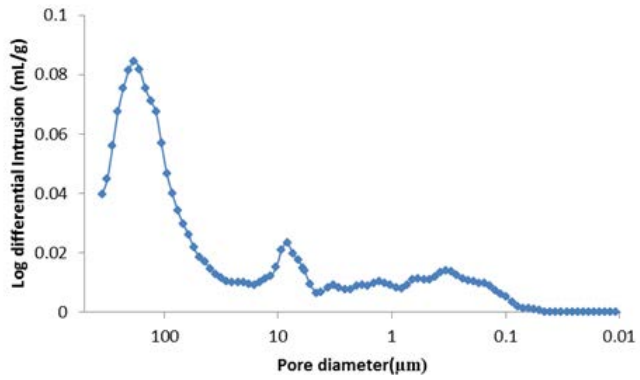

Fig. 16. Pore size distribution of supports containing 4 wt.% of Alc sintered at 1,350°C for 2 h.

3.2.7. Water permeability

Figs. 18 and 19 show the results of the evaluation of water permeability. The flux has a linear evolution in function of the pressure and the percentage of aluminum. Hence, the hydraulic permeability showed approximately a ten-fold increase after the addition of 4 wt.% of aluminum to the mixture. Indeed, the 4 wt.% addition of Ali boosted the permeability from 4.673 to 42.944 L h^{-1} m^{-2} bar^{-1} at a pressure of 6 bar. Similarly, the 4 wt.% addition of Alc resulted in a permeability of 38.339 L h^{-1} m^{-2} bar^{-1} at the same pressure. Then, the hydraulic permeability continued to rise steadily with the increase of aluminum percentage and the pressure to reach 147.56 and 141.91 L h^{-1} m^{-2} bar^{-1} with the addition of 20 wt.% of Ali and Alc, respectively. As was demonstrated in ref. [24] in an earlier work, an increase of metal contents to the porcelain supports causes a higher flux. This is probably due to the exothermic oxidation reaction of aluminum which can produce germination of the α-alumina phase that can react with the metal-kaolin to produce porous mullite. This reaction gives rise to bigger voids and pores in the elaborated cermet supports. In addition, our study confirms ref. [25] in their explanation of this increase in permeability by the increase in the amount of interconnected pores created by aluminum burnout in the ceramic supports over the thermal treatment.

However, the slight difference in permeability between membranes with Ali and those with Alc can be explained by the presence of impurities in Ali that are burned out during heat treatment leaving in their places more pores.

3.2.8. Implementation of the membrane for paper mill wastewater treatment

Two membranes, one containing 4 wt.% of Ali and another containing 4 wt.% of Alc, were used to treat wastewater from paper mills. Fig. 20 presents the variation of permeate flux of wastewater from paper mill sintered at 1,350°C for 2 h (T = 25°C, TMP = 6 bar). As it can be seen for the two membranes, flux decreases with the time. This can be attributed to the fouling phenomenon which increases by the use of dead-end filtration. This behavior was explained by the pore blockage and cake filtration phenomena at the surface of the membrane due to the interaction between membrane material and effluent which stabilizes the flux [26]. As a consequence, it does not reach zero.

Table 5 reveals that using the colorimetric method, the microfiltration through the support membrane containing 4 wt.% of Alc proved to be very efficient in removing the chemical oxygen demand (COD). Indeed, the content in COD dropped from 5,700 to 175 mg L^{-1} and to 569 mg L^{-1} after filtering the waste by the support membrane containing 4 wt.% of Alc and one containing 4 wt.% of Ali, respectively. Furthermore, the use of Turbidimeter allowed to record a

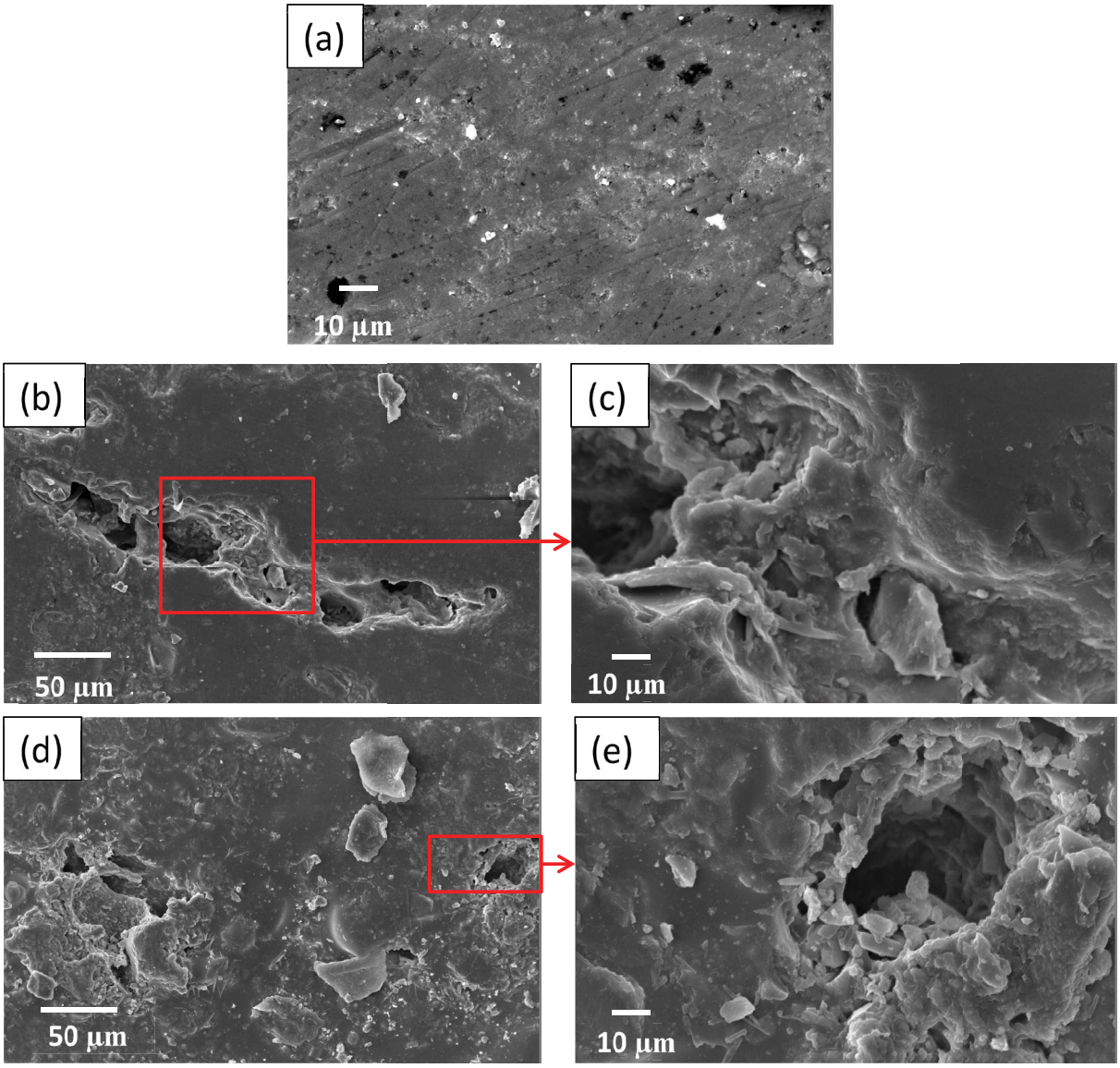

Fig. 17. SEM micrographs of the samples sintered at 1,350°C for 2 h with different percentages of aluminum: support containing 0 wt.% of Al (a), support containing 4 wt.% of Ali (b) and (c), and support containing 4 wt.% of Alc (d) and (e).

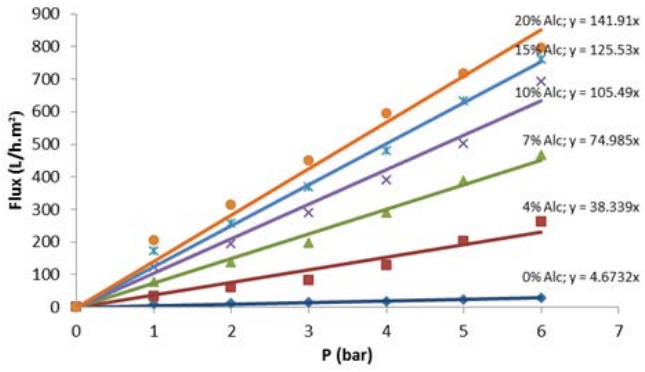

Fig. 18. Water permeability of the different samples containing various weight percentages of Alc after sintering at 1,350°C for 2 h.

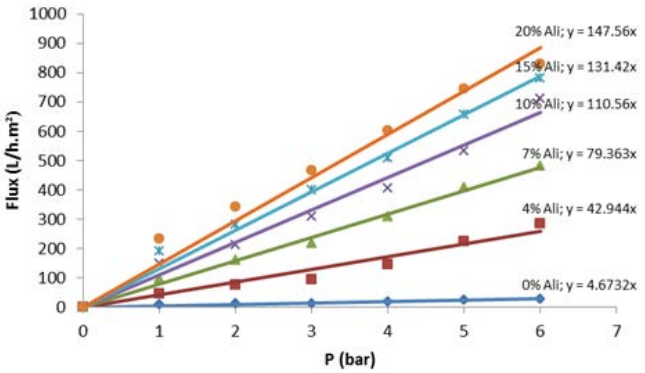

Fig. 19. Water permeability of the different samples containing various weight percentages of Ali after sintering at 1,350°C for 2 h.

very clear improvement of the turbidity of the treated water. The support membrane containing 4 wt.% of Alc dropped the turbidity of the wastewater from 329 to 50.4 NTU. Equally, the support membrane containing 4 wt.% of Ali dropped the same value to 78.4 NTU. Fig. 21 presents photos illustrating the obvious improvement of color removal from the wastewater filtered by membranes containing 4 wt.% of aluminum. Nevertheless, despite the improvement in conductivity and salinity, the obtained results would not be considered satisfactory.

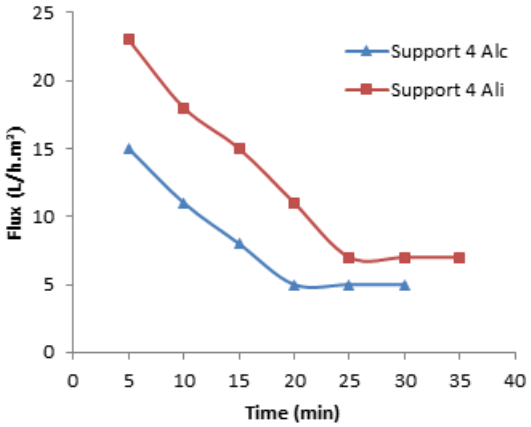

Fig. 20. Variation of permeate flux with time (T = 25°C, TMP = 6 bar).

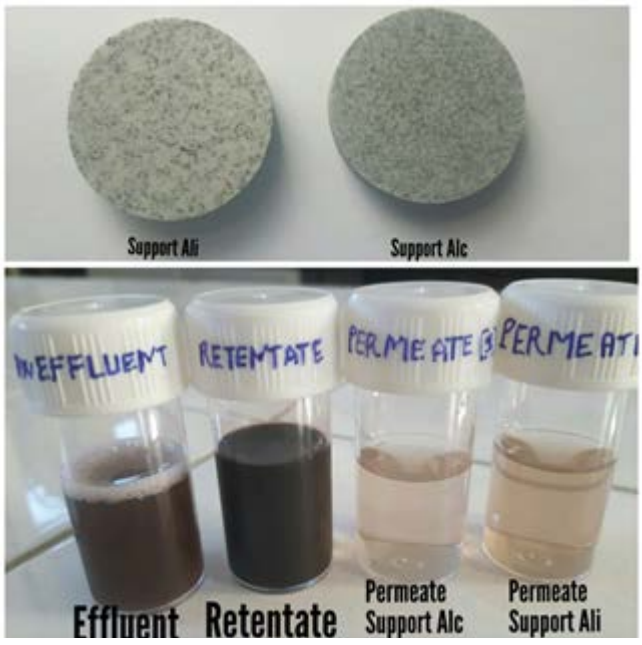

Fig. 21. Photographs of the membrane supports sintered at 1,350°C for 2 h and the paper mill effluent before and after treatment.

3.2.9. Comparison of membrane supports

Compared with organic membranes, inorganic membranes have been used extensively in many industrial processes, notably to solve some environmental problems, such as water and effluent treatments [27–28], gas purification [29], and protection of aquaculture basins [30]. In this study, porous ceramic supports for filtration membrane were successfully fabricated via kaolin and aluminum powders. In terms of price, the cost of support containing Alc is higher than the support prepared by the aluminum waste (Ali) since 1 kg of Alc is purchased from Fluka (Spain) at €250 while Ali is provided at no cost from local companies which dispose it as a waste. It can be said that the support containing aluminum waste is economical, environmental friendly, and does not need any further processing before using it, making it a better choice as an additive to ceramics for the fabrication of cermet membranes to be implemented in paper mill wastewater treatment.

4. Conclusions

This study reported on the elaboration and the characterization of flat cermet membrane supports based on kaolin and aluminum powder mixtures produced by dry molding. It revealed that the addition of 4 wt.% of Alc or Ali would be very beneficial to the improvement of the mechanical characteristics, especially in terms of resistance. In addition, the addition of the metal would increase the porosity of the membranes. Furthermore, the work reported on the implementation of the designed membranes in the treatment of paper mill wastewater. It showed that there were very promising results in removing COD, reducing turbidity, and improving the color of the treated wastewaters. Finally, the work compared the performance of the membranes with Alc with that with Ali. The tests revealed a slight better performance of the former. However, because of the abundance of waste aluminum and its low cost, it would be much more beneficial to use it as an additive to kaolin instead of Alc. Hence, the optimum conditions recommended by this work for an efficient and environmental-friendly membrane would contain 4 wt.% aluminum. The recommended optimum operational conditions that would yield the best results with a cermet containing 4 wt.% of Ali would be a temperature of 25°C and a pressure equal to 6 bar. Nevertheless, further

Table 5
Characteristics of the effluent before and after filtration

Sample	Conductivity (μS cm^{-1})	Turbidity (NTU)	COD (mg L^{-1})	Salinity (g L^{-1})
Raw effluent	1,984 ± 0.3	329 ± 0.2	5,700 ± 0.3	1.3 ± 0.1
The support membrane containing 4 wt.% of Alc	1,556 ± 0.3	50.4 ± 0.2	175 ± 0.1	1.1 ± 0.1
The support membrane containing 4 wt.% of Ali	1,727 ± 0.2	78.4 ± 0.1	569 ± 0.1	1.2 ± 0.1

studies are still needed for the preparation of a better tubular cermet membrane with better filtration efficiency.

Acknowledgments

This study was supported financially by the Ministry of Higher Education and Scientific Research of Tunisia. Moreover, the authors would like to thank ENSCI (Ecole Nationale Supèrieure de Céramique Industrielle), University of Limoges, France, for their collaboration. The authors would also like to extend their thanks to Dr Ayadi Hajji for proofreading, editing, and correcting the English of the manuscript.

References

[1] S.J. Yoo, H.S. Yoon, H.D. Jang, S.T. Hong, H.S. Park, S.U. Park, D.H. Kwak, S.I. Lee, Synthesis of aluminum et hoxide from used aluminum cans, Korean J. Chem. Eng., 24 (2007) 872–876.
[2] CEN, Aluminium and Aluminium Alloys: Terms and Definitions—Part 3: Scrap; EN 12258; CEN: Brussels, Belgium, 2013, p. 2.
[3] International Minerals Statistics and Information (USGS). Available online: http://minerals.usgs.gov/ minerals/pubs/ country/ (accessed on 15 February 2018).
[4] T.V. Gestel, C. Vandecasteele, A. Buekenhoudt, C. Dotremont, J. Luyten, R. Leysen, B.V. der bruggen, G. Maes, Alumina and titania multilayer membranes for nanofiltration: preparation, characterization and chemical stability, J. Membr. Sci., 207 (2002) 73–89.
[5] N.P. Xu, W.H. Xing, Y.J. Zhao, Separation technology and application of inorganic membrane, Chem. Ind., 25 (2003) 230–237.
[6] R.D. Sahnoun, S. Baklouti, Characterization of flat ceramic membrane supports prepared with kaolin-phosphoric acid-starch, Appl. Clay Sci., 83–84 (2013) 399–404.
[7] A. Harabi, F. Zenikheri, B. Boudaira, F. Bouzerara, A. Guechi, L. Foughali, A new and economic approach to fabricate resistant porous membrane supports using kaolin and $CaCO_3$, J. Eur. Ceram. Soc., 34 (2014) 1329–1340.
[8] J. Fang, G. Qin, W. Wei, X. Zhao, L. Jiang, Elaboration of new ceramic membrane from spherical fly ash for microfiltration of rigid particle suspension and oil-in water emulsion, Desalination, 311 (2013) 113–126.
[9] R.D. Colle, C. Fortulan, S.R. Fontes, Manufacture and characterization of ultra and microfiltration ceramic membranes by isostatic pressing, Ceram. Int., 37 (2011) 1161–1168.
[10] S. Jana, M.K. Purkait, K. Mohanty, Preparation and characterization of low-cost ceramic microfiltration membranes fort the removal of chromate from aqueous solutions, Appl. Clay Sci., 47 (2010) 317–324.
[11] Y. Dong, X. Feng, D. Dong, S. Wang, J. Yang, J. Gao, X. Liu, G. Meng, Elaboration and chemical corrosion resistance of tubular macro-porous cordierite ceramic membrane supports, J. Membr. Sci., 304 (2007) 65–75.
[12] B.K. Nandi, R. Uppaluri, M.K. Purkait, Preparation and characterization of low cost ceramic membranes for micro-filtration applications, Appl. Clay Sci., 42 (2008) 102–110.
[13] H.J. Yeom, S.C. Kim, Y.W. Kim, I.H. Song, Processing of alumina-coated clay diatomite composite membranes for oily wastewater treatment, Ceram. Int., 42 (2016) 5024–5035.
[14] G. Cizeron, Métallurgie des poudres, La revue de métallurgie CIT 5, 1994, pp. 683–692.
[15] X. Meng, J. Song, N. Yang, B. Meng, X. Tan, Z.F. Ma, K. Li, Ni–$BaCe_{0.95}Tb_{0.05}O_{3-\delta}$ cermet membranes for hydrogen permeation, J. Membr. Sci., 401 (2012) 300–305.
[16] C. Zuo, T.H. Lee, S.E. Dorris, Composite Ni–Ba $(Zr_{0.1}Ce_{0.7}Y_{0.2})O_3$ membrane for hydrogen separation, J. Power Sources, 159 (2006) 1291–1295.
[17] H. Kim, B. Kim, J. Lee, K. Ahn, H.R. Kim, K.J. Yoon, J.H. Lee, Microstructural adjustment of Ni–$BaCe_{0.9}Y_{0.1}O_{3-\delta}$ cermet membrane for improved hydrogen permeation, Ceram. Int., 40 (2014) 4117–4126.
[18] M. Samuel, A new technique for recycling aluminium scrap, J. Mater. Process. Technol., 135 (2003) 117–124.
[19] J.B. Fogagnolo, E.M. Ruiz-Navas, M.A. Simón, M.A. Martinez, Recycling of aluminium alloy and aluminium matrix composite chips by pressing and hot extrusion, J. Mater. Process. Technol., 143–144 (2003) 792–795.
[20] S. Timoshenko, J.N. Goodier, Theory of elasticity, Urmo, Bilbao, 1975.
[21] A. Yamuna, S. Devanarayanan, M. Lalithambika, Phase-Pure Mullite from Kaolinite, J. Am. Ceram. Soc., 85 (2002) 1409–1413.
[22] T. Ebadzadeh, Porous mullite-ZrO_2 composites from reaction sintering of zircon and aluminum, Ceram. Int., 31 (2005) 1091–1095.
[23] V. Viswabaskaran, F.D. Gnanam, M. Balasubramanian, Mullitisation behaviour of south Indian clays, Ceram. Int., 28 (2002) 557–564.
[24] M. Issaoui, J. Bouaziz, M. Fourati, Elaboration of membrane ceramic supports using aluminum powder, Desal. Wat. Treat., 53 (2015) 1037–1044.
[25] M. Issaoui, L. Limousy, B. Lebeau, J. Bouaziz, M. Fourati, Design and characterization of flat membrane supports elaborated from kaolin and aluminum powders, C.R. Chim., 19 (2016) 496–504.
[26] Q. Han, W. Li, T.A. Trinh, X. Liu, J.W. Chew, A network-based approach to interpreting pore blockage and cake filtration during membrane fouling, J. Membr. Sci., 528 (2017) 112–125.
[27] K. Ramesh, C. Sankha, P. Parimal, Membrane-integrated physicochemical treatment of coke-oven wastewater: transport modelling and economic evaluation, Environ. Sci. Pollut. Res., 22 (2015) 6010–6023.
[28] L. Jian, H. Zhen, Development of a dynamic mathematical model for membrane bio electrochemical reactors with different configurations, Environ. Sci. Pollut. Res., 23 (2016) 3897–3906.
[29] N.W. Jusoh, K.K. Lau, A.M. Shariff, Purification of natural gas with impurities using membrane processes: parameter estimation, Am. J. Eng. Appl. Sci., 5 (2012) 78–83.
[30] J.B. Castaing, A. Massé, V. Séchet, N.E. Sabiri, M. Pontié, J. Haure, P. Jaouen, Immersed hollow fibres microfiltration (MF) for removing micro-algae and protecting semi-closed aquaculture basins, Desalination, 276 (2011) 386–396.